# Ground Response in Lotung: Total Stress Analyses and Parametric Studies

Ronaldo I. Borja[1]; Blaise G. Duvernay[2]; and Chao-Hua Lin[3]

**Abstract:** Previous papers have reported on the performance of a recently developed nonlinear ground response analysis code, *SPECTRA*, with reference to the prediction of the free-field response at a Large-Scale Seismic Test site in Lotung, Taiwan during the M6.5 earthquake of May 20, 1986. Two more major earthquakes of different characteristics shook this test site later that same year, a M6.2 earthquake that occurred on July 30 and a M7.0 earthquake that occurred on November 15. The present article analyzes the free-field responses recorded by a downhole array from these latter two events using the code *SPECTRA* and a widely used equivalent linear analysis code *SHAKE*. The studies focus on the relative accuracy and sensitivity of the two codes with respect to the variations of the input material parameters, using time histories, acceleration response spectra, Fourier acceleration amplitude spectra, and Arias intensities as criteria for the comparison. The two codes captured the general wave form of the acceleration histories well, but there was a general tendency for both codes (particularly *SHAKE*) to underpredict the Arias intensities of the earthquakes.

**DOI:** 10.1061/(ASCE)1090-0241(2002)128:1(54)

**CE Database keywords:** Stress analysis; Bounding surface; Finite element method; Ground motion; Plasticity.

## Introduction

Lotung is a seismically active region in the northeastern part of Taiwan, and was the site of a strong motion Large-Scale Seismic Test (LSST) instrumentation system installed by the Electric Power Research Institute, in cooperation with Taiwan Power Company, for soil-structure interaction research. One of the instrumentation arrays consisted of a set of downhole three-component accelerometers extending to a depth of 47 m, known as the downhole B (DHB) array. The role of the DHB array is to monitor free-field responses resulting from seismic activities at the LSST site. On May 20, 1986, a M6.5 earthquake shook the test site (denoted as the LSST7 event). This seismic event has been investigated extensively by a number of researchers, and the recordings of the DHB array have been analyzed and simulated many times using different site response analysis codes (Chang et al. 1990; Lee and Finn 1992; Li et al. 1992; Pyke 1992; Borja et al. 1999a, 2000).

Soon after the LSST7 event, more than 20 pore pressure transducers have been installed and synchronously wired to the accelerometer arrays at the LSST site (Shen et al. 1989). These sensors served to monitor seismically-induced pore pressure activities at the test site, and were embedded at depths varying from 3 to 16 m where the soils are known to be fluid-rich and potentially liquefiable. Two more major earthquakes shook the test site later that same year, a M6.2 earthquake on July 30 (LSST12 event) and a M7.0 earthquake on November 30 (LSST16 event). In both events, the measured excess pore pressures were in the order of about 25% of the initial vertical effective stress, by no means insignificant but still well below the level necessary to cause liquefaction (Li et al. 1998). The objective of the present paper is to analyze the recorded free-field responses generated by the latter two earthquakes using two site response analysis codes that employ a total stress formulation. In a separate work (Lin and Borja 2000), an alternative modeling approach based on effective stresses is used to predict the excess pore pressures that developed at the test site.

A number of site response analysis codes have been developed in the past to simulate the effects of soil condition on strong ground motion (Schnabel et al. 1972; Lee and Finn 1991; Li et al. 1992; Pyke, 1992; Borja et al. 1999a). A comparison of the predictive capabilities of some of these codes is presented in an Electric Power Research Institute (EPRI) Report (Electric 1993). Recently, Borja et al. (2000) compared five different site response analysis codes in terms of how accurately they predicted the ground responses resulting from the LSST7 event. The acceleration profiles that resulted from the LSST7 event were not as irregular as those generated by either the LSST12 or LSST16 event, and higher-frequency modes were not as dominant. Hence, it is worthwhile to re-investigate the accuracy of these codes to see how well they can predict more complex earthquake ground responses. Page limitations prohibit the present article from being exhaustive, so we simply consider two site response analysis codes that have similar features and yet are so algorithmically different in the manner in which they compute the ground motion responses. In this article, we compare a recently developed nonlinear finite element (FE) code *SPECTRA* (Borja et al. 1999a) with a widely used equivalent linear analysis code *SHAKE* (Schnabel et al. 1972).

[1]Associate Professor, Dept. of Civil and Environmental Engineering, Terman Engineering Center, Stanford Univ., Stanford, CA 94305-4020. E-mail: borja@cive.stanford.edu

[2]Graduate Student, Dept. of Civil and Environmental Engineering, Stanford Univ., Stanford, CA 94305.

[3]Graduate Student, Dept. of Civil and Environmental Engineering, Stanford Univ., Stanford, CA 94305.

Note. Discussion open until June 1, 2002. Separate discussions must be submitted for individual papers. To extend the closing date by one month, a written request must be filed with the ASCE Managing Editor. The manuscript for this paper was submitted for review and possible publication on June 28, 2000; approved on May 24, 2001. This paper is part of the ***Journal of Geotechnical and Geoenvironmental Engineering***, Vol. 128, No. 1, January 1, 2002. ©ASCE, ISSN 1090-0241/2002/1-54–63/$8.00+$.50 per page.

Both *SHAKE* and *SPECTRA* are formulated in terms of total stresses, so neither code is capable of predicting the excess pore pressures that build up in fluid-saturated soils during seismic shaking. However, they have algorithmically contrasting approaches to computing earthquake ground responses, because whereas *SHAKE* uses an equivalent linear analysis approach, *SPECTRA* is a truly nonlinear model, and while *SHAKE* formulates the problem in the frequency domain, *SPECTRA* integrates the solution in the time domain. Still, despite these fundamental differences, the two codes rely basically on the same input material information to make numerical predictions, namely, the elastic shear modulus profiles, as well as the shear modulus-shear strain degradation curve for the soil. In addition, *SHAKE* requires a damping ratio-shear strain curve, whereas *SPECTRA* only needs the asymptotic value of this curve in the limit of zero-shear strain. Thus, *SPECTRA* effectively requires less material information than *SHAKE*; nevertheless, both codes are subject to the same variations in the input material parameters.

Unlike the elastic moduli of the soil which can be estimated reliably from geophysical seismic tests, accurate moduli ratio and damping ratio curves are difficult to develop in practice because they are usually inferred from laboratory test results, which, in turn, are influenced to a great extent by sample disturbance effects and bias in the laboratory testing procedures. For example, sudden jumps in the moduli and damping ratio values from those obtained by resonant column testing to those obtained by cyclic triaxial testing are not uncommon (Tang et al. 1990; Borja and Amies 1994). These uncertainties have led to the development of a technique to back-figure material properties from the earthquake site responses themselves (Zeghal et al. 1995), but even this procedure naturally produces scattering of data points. This suggests that when performing site response analyses, one should naturally expect to deal with a band of possible material property values, and not a unique curve. This article reports how well the two site response analysis codes handled the problem of variations in the material properties in Lotung with respect to the prediction of the ground responses resulting from the LSST12 and LSST16 events.

## Comparison of Algorithms

*SHAKE* is an equivalent linear analysis computer code developed to analyze the problem of vertically propagating shear waves through a linear viscoelastic system (Schnabel et al. 1972). To account for the nonlinearity of soil behavior, the computer program iterates to find an effective shear strain which gives equivalent secant shear modulus and equivalent linear damping ratio that best approximate the actual nonlinear hysteretic stress–strain behavior of cyclically loaded soils. The program requires a profile of elastic shear modulus in all soil layers, as well as a curve, or a set of curves, that shows how the shear modulus degrades with increasing shear strain (Hardin and Drnevich 1972). The model does not explicitly distinguish between plastic hysteretic damping and viscous damping, but instead simply considers all damping as viscous in nature. Hence, the code also requires a curve, or a set of curves, that characterizes how the damping ratio increases with shear strain. Despite the iterations required to find the effective shear strain, *SHAKE* is still a linear analysis program and, therefore, can not predict permanent deformations.

*SPECTRA* is a nonlinear FE program developed to analyze the problem of vertically propagating shear and longitudinal waves through a viscous, elastoplastic soil medium (Borja et al. 1999a). To account for the kinematical constraints of vertically propagating waves, as well as the coupled deformations induced by the three components of motion, special ''stick'' finite elements have been developed. The program explicitly distinguishes between viscous damping and plastic hysteretic damping through the assumption that the stresses decompose additively into viscous and inviscid parts. The inviscid component of the constitutive model is facilitated by a bounding surface theory with a vanishing elastic region (Borja and Amies 1994), which predicts instantaneously elastic response in the limit of zero strains. The algorithm integrates the equations of motion in time domain either by the Newmark method or the $\alpha$-method of Hilber et al. (1977).

Inside the bounding surface, the program interpolates the plastic hardening modulus exponentially using two parameters, $h$ and $m$, which are obtained from the moduli ratio-shear strain curve. Since the model formulation assumes that the latter curve can be represented by the values of the parameters $h$ and $m$ alone, only two points on the moduli ratio-shear strain curve must be input to completely define the inviscid component of the constitutive model. *SPECTRA* does not require the damping ratio curve, except for the zero-shear-strain asymptote of this curve which describes the viscous component of the hysteretic response. The idea is that any truly hysteretic model should be able to generate the effects implied by the damping ratio-shear-strain relationship from the shape of the hysteretic response implied by the moduli ratio-shear strain curve. However, *SPECTRA* does require that a value of dominant frequency of the input motion be estimated either from the input response spectra or Fourier amplitude response spectra to construct the viscous damping matrix.

## Description of Large Scale Seismic Test Site and Soil Data

Lotung was the site of two scaled-down nuclear plant containment structures (1/4-scale and 1/12-scale models) constructed for soil–structure interaction research. Fig. 1 shows the location of the surface accelerometers and two downhole instrumentation arrays in the vicinity of the 1/4-scale nuclear containment model. Free-field array DHB is located at about 49 m horizontally from the edge of the model and contain three-component downhole accelerometers oriented in the east–west (EW), north–south (NS), and up–down (UD) directions installed at depths of 0, 6, 11, 17, and 47 m from the ground surface. The accelerometers are denoted as FA1-5, DHB6, DHB11, DHB17, and DHB47, respectively. Accelerometer DHB47 was operational during the LSST7 event but not during the LSST12 and LSST16 events.

In addition to the surface and downhole accelerometers, a total of 27 pore pressure transducers have been installed in clusters at the test site to monitor seismically-induced pore pressure activities as shown in Fig. 1. Some of these sensors were fully operational during the LSST12 and LSST16 events, but have not been installed early enough for the LSST7 event. A detailed description of the pore pressure recording system can be found in Shen et al. (1989). An analysis of the recorded pore pressure data using an effective stress model that employs an ellipsoidal bounding surface constitutive theory (Borja et al. 2001) is presented in a separate work (Lin and Borja 2000).

Shear and compression wave velocities determined from seismic crosshole and uphole tests have been used to describe the elastic material properties of the soil at the test site (Anderson and Tang 1989). A description of the variations of the elastic soil properties with depth can be found in Borja et al. (1999a, 2000). Within the upper 17 m of the soil deposit, the shear wave velocity varies linearly from about 100 m/s at the surface to about 200 m/s

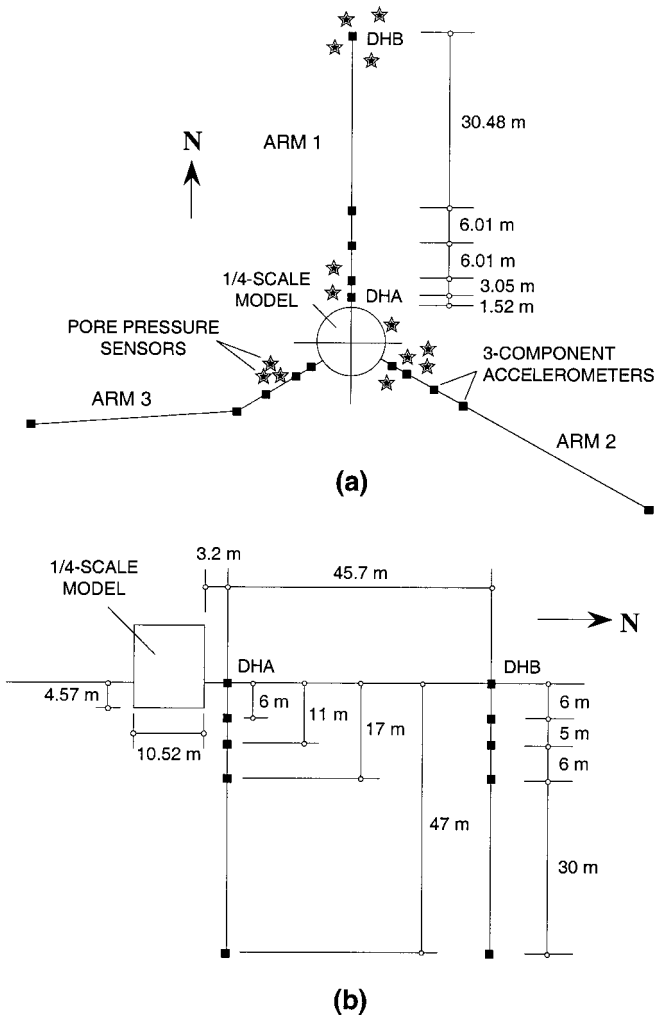


**Fig. 1.** Location of surface and downhole instrumentation, Large-Scale Seismic Test site: (a) plan; (b) elevation

at 17 m depth. Statistically, the variation of the measured shear wave velocities is very small [see Fig. 3(a) of Borja et al. (1999a)], and is thus ignored in the parametric studies.

The greatest uncertainties lie in the variations of the moduli ratio and damping ratio with shear strain. Moduli and damping ratio data on soil specimens from Lotung have been reported by Anderson and Tang (1989). Unfortunately, these data did not properly convert axial strains to shear strains, which had been discovered only after the EPRI proceedings were published. Stokoe (Electric 1993) also conducted some very careful resonant column and cyclic torsion tests on ''undisturbed'' soil specimens from Lotung. Results of these tests (conducted at the University of Texas, Austin) are shown in Fig. 2. The moduli ratio data of Stokoe conform fairly well to the upper bound curve proposed by Seed and Idriss (1970) for sand (shaded region in Fig. 2), while the material damping ratio data fall between the mean and lower bounds of the Seed–Idriss curves.

In order to avoid bias with laboratory testing procedures and sample disturbance effects, Zeghal et al. (1995) back-figured the moduli and damping ratio curves from the acceleration-time histories recorded by instruments DHB6, DHB11, and DHB17 during the LSST7, LSST12, and LSST16 events. The technique adopted by Zeghal et al. (1995) is to integrate twice the acceleration-time histories to obtain the absolute displacements, and then finite difference the depth to obtain the corresponding shear strain-time histories. The Zeghal et al. technique also uses a one-dimensional beam idealization to generate the corresponding shear stress-time histories. Results of their analyses are shown in Fig. 3 for the three earthquakes, along with the bands for sands proposed by Seed and Idriss (1970). Also shown in Fig. 3 are the upper bound (UB), lower bound (LB), and statistical fit (SF) curves used by Borja et al. (2000) for their parametric studies of the LSST7 ground motion data. Note that the term ''upper bound'' is defined by Borja et al. to refer to the stiffer material response, and thus for the damping ratio values, this term effectively pertains to the LB.

The data shown in Fig. 3 suggest that the band of moduli ratio values developed by Seed and Idriss for sands conforms very well with the band used by Borja et al. (2000) for their parametric studies of the LSST7 ground motion data at 6 and 11 m depths, but tends to be on the UB side at 17 m depth. On the other hand, the Seed–Idriss band for damping ratio tends to be on the UB side of the Borja et al. band for all the three depths considered. Fur-

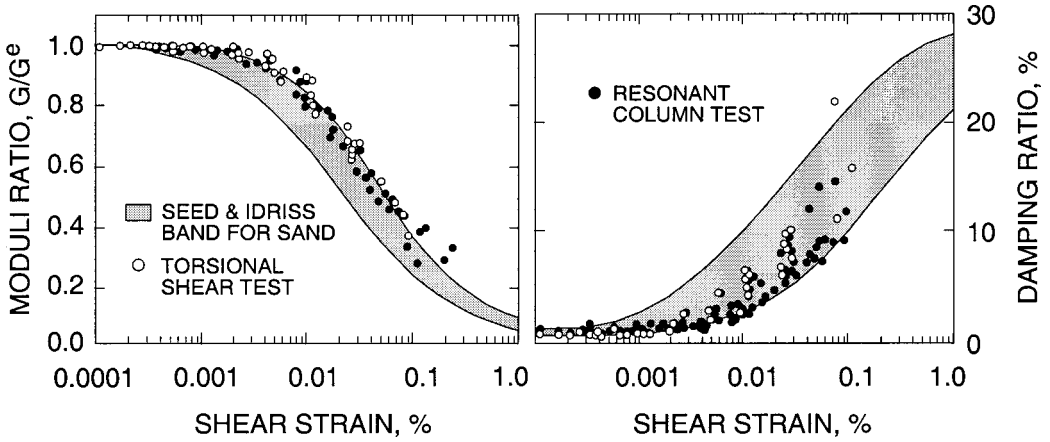


**Fig. 2.** Moduli and damping ratio curves for Large-Scale Seismic Test case study: Torsional shear and resonant column tests (Electric 1993) and band for sands proposed by Seed and Idriss (1970)

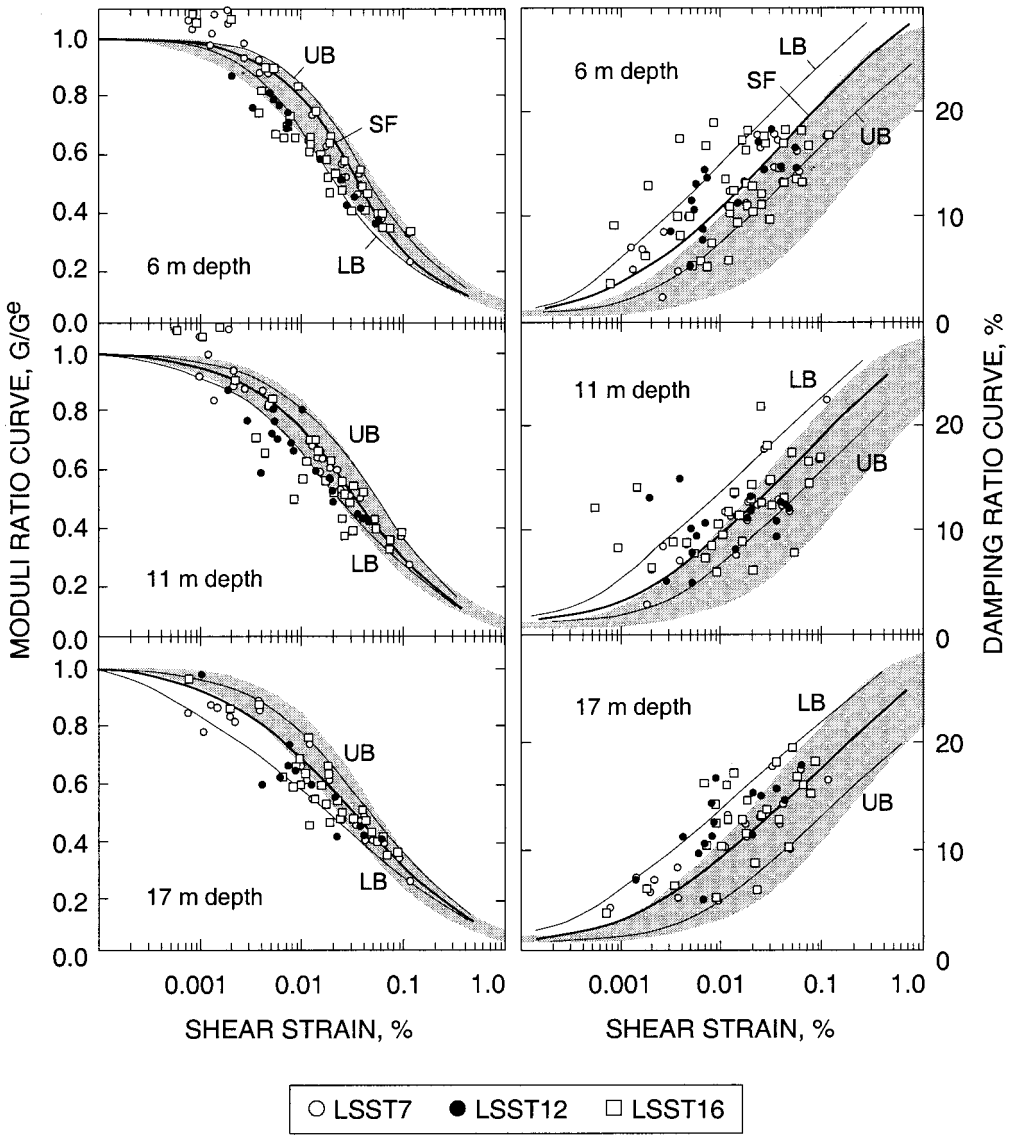


**Fig. 3.** Moduli and damping ratio curves for Large-Scale Seismic Test case study: UB=upper bound; SF=statistical fit; LB=lower bound; shaded region=band for sands proposed by Seed and Idriss (1970)

thermore, the Borja et al. band developed to study the LSST7 event appears to be appropriate for the LSST12 and LSST16 events as well, and hence will also be used for the present parametric studies. The accuracy of the Zeghal et al. (1995) approach for back-figuring soil properties directly from the earthquake ground responses is a function of the downhole instrument spacing and recorded acceleration wavelengths, and for the Lotung site, the approximation errors are estimated by Zeghal et al. to be less than 2%.

## Comparison of Three Earthquakes

Table 1 compares the three major earthquakes that shook the LSST site in 1986. LSST16 recorded the highest magnitude at 7.0, but it also had the greatest epicentral distance at 80 km. In terms of the peak ground acceleration (PGA) recorded by accelerometer FA1-5, LSST7 registered the highest PGA in both the EW and NS directions, but LSST12 registered the highest PGA in

**Table 1.** Comparison of 1986 Lotung Earthquakes as Recorded on FA1-5. Bracketed Duration Based on Threshold Accelerations of 0.05 g for East–West and North–South, 0.02 g for Up–Down; Number of Zero Crossings/Sec Calculated Over Bracketed Duration

| Event | LSST7 | LSST12 | LSST16 |
|---|---|---|---|
| Date | 5/20/86 | 7/30/86 | 11/14/86 |
| Magnitude $M_w$ | 6.5 | 6.2 | 7.0 |
| Epicentral distance, km | 66 | 6 | 80 |
| Focal depth, km | 15.8 | 1.6 | 6.9 |
| PGA, EW, g | 0.156 | 0.155 | 0.130 |
| PGA, NS, g | 0.207 | 0.190 | 0.170 |
| PGA, UD, g | 0.041 | 0.195 | 0.095 |
| Bracketed duration, EW, s | 8.52 | 2.98 | 13.04 |
| Bracketed duration, NS, s | 9.58 | 2.70 | 19.44 |
| Bracketed duration, UD, s | 9.16 | 5.30 | 31.08 |
| No. zero crossings/s, EW | 3.6 | 6.7 | 5.2 |
| No. zero crossings/s, NS | 3.1 | 7.8 | 4.8 |
| No. zero crossings/s, UD | 4.0 | 18.5 | 10.0 |

the vertical direction. The relative complexities of the three earthquakes may be compared by prescribing threshold accelerations, in this case, 0.05 g for the EW and NS directions and 0.02 g for the UD direction, and measuring the bracketed duration (Bolt 1969) representing the time between the first and last exceedances of these threshold accelerations. The number of zero crossings per second is then computed over this bracketed duration to describe the complexity of the earthquake.

As mentioned in the Introduction, the previously studied LSST7 earthquake was not as irregular as the LSST12 and LSST16 earthquakes. This can be inferred from the results shown in Table 1 which reveal that the latter two earthquakes registered more zero crossings per second over the corresponding bracketed durations. Specifically, the LSST16 earthquake recorded the longest bracketed duration and the most number of zero crossings, implying the most number of significant load or stress reversals during this bracketed period. In the next section, we describe how well the two codes predicted the more irregular LSST12 and LSST16 ground motions using acceleration-time histories, acceleration response spectra, Fourier acceleration amplitude spectra, and Arias intensities as criteria for the comparison.

## Results and Discussions

The analysis procedure follows a similar approach to that described in Borja et al. (2000). First, UB and LB curves, as well as SF curves, were generated for the moduli and damping ratio variations with shear strain, as shown in Fig. 3. From a practical standpoint, it was not realistic to attempt to envelop all the data points back-figured by Zeghal et al. (1995) from the three earthquakes, so we use the same band of soil properties previously considered by Borja et al. for the LSST7 studies (Fig. 3) to study the LSST12 and LSST16 ground motions. This appears to be a realistic compromise between the Zeghal et al. data points for all the three earthquakes which mildly cluster toward the LB curves of Borja et al. (Fig. 3), and the data points from laboratory tests (Fig. 2) which tend to cluster toward the UB curves. Ground motions recorded by DHB17 were input at 17 m depth, and surface ground motions were calculated. For *SPECTRA*, the three components of motion were input simultaneously, while for *SHAKE*, the two horizontal components were analyzed separately.

For *SHAKE*, EW and NS time histories were prescribed separately at 17 m depth and the corresponding acceleration-time histories were computed on the ground surface. Toward this end, the SF, UB, and LB shear modulus and damping ratio curves were generated into separate *SHAKE* input files, point by point. A cutoff frequency of 25 Hz was used, and the ratio of effective to maximum shear strain was adjusted according to the recommendation of Idriss and Sun (1992). For *SPECTRA*, the model parameters $R$, $\tau_{max}$, $H_0$, $h$, and $m$ are the same as those used in Borja et al. (2000). The viscous damping ratio determined from the asymptotic zero-shear-strain value is equal to $\xi_0 = 1\%$, while the dominant frequency used to construct the damping matrix was estimated as 0.7 Hz for both LSST12 and LSST16 earthquakes. Stick FE's 1 m long were used to discretize the soil layer. A time-integration algorithm based on the $\alpha$-method of Hilber et al. (1977) was employed with the following time-integration parameters: $\beta = 0.3025$, $\gamma = 0.60$, and $\alpha = -0.10$; the time increment is $\Delta t = 0.01$ s. Borja et al. (1999a, 1999b) have shown that these values are sufficient for the FE discretization and the soil profile in Lotung.

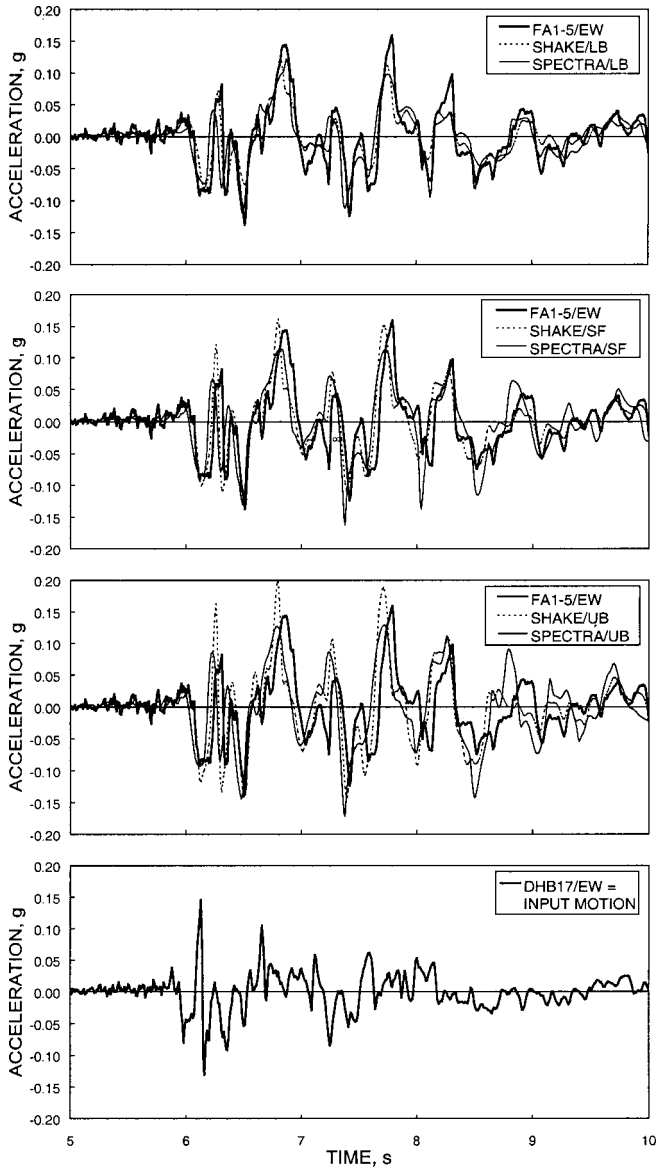


**Fig. 4.** EW ground surface acceleration-time history using *SHAKE* and *SPECTRA*: Lotung LSST12 case study

### Horizontal Acceleration-Time Histories

Figs. 4 and 5 show EW and NS ground surface acceleration-time histories predicted by *SHAKE* and *SPECTRA*, as well as the corresponding records obtained by surface instrument FA1-5 for the LSST12 event. The input motions at 17 m depth are also shown. Note that the peak values predicted by *SHAKE* increase monotonically with UB approximations to the moduli and damping ratio values, a typical feature of an equivalent linear analysis solution. However, the same is not true of the predictions by the nonlinear code *SPECTRA* which shows that the primary peak values do not necessarily increase, while the secondary peak values are the ones that amplify more with UB approximations. Qualitatively, neither code predicted the recorded ground surface motions very well even with the use of the SF curves. This could have been due to the fact that LSST12 was a shallower and near-fault earthquake (see Table 1), causing inclined waves to have a much more significant impact on the recorded ground response (Kramer 1996).

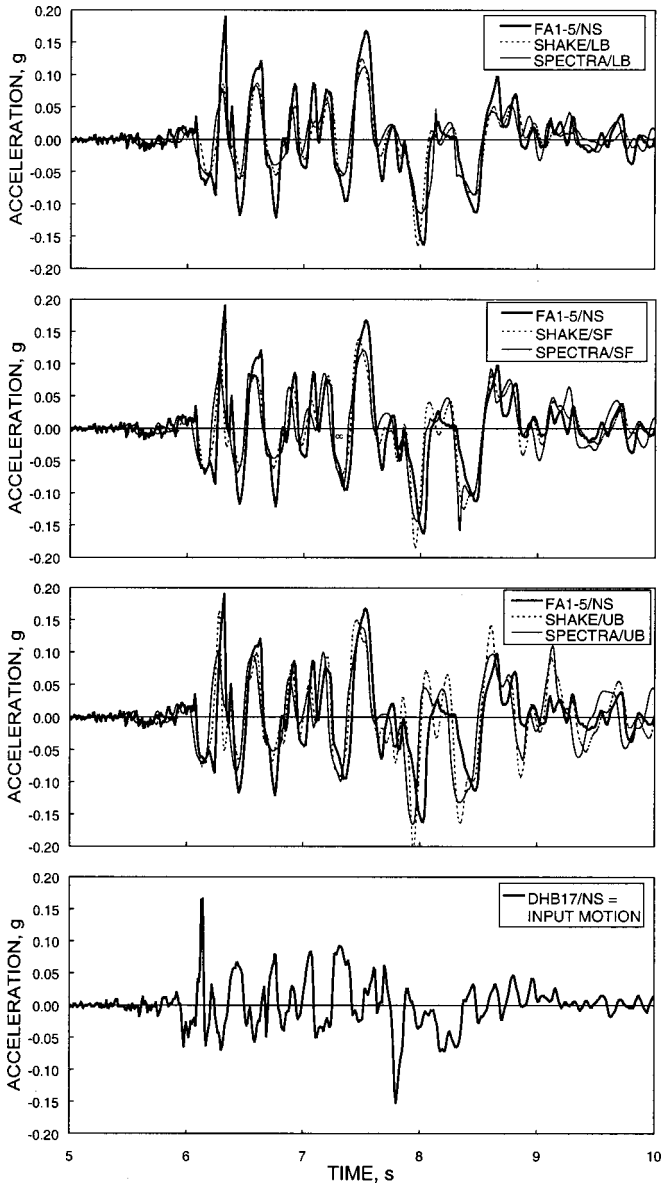


**Fig. 5.** NS ground surface acceleration-time history using *SHAKE* and *SPECTRA:* Lotung LSST12 case study

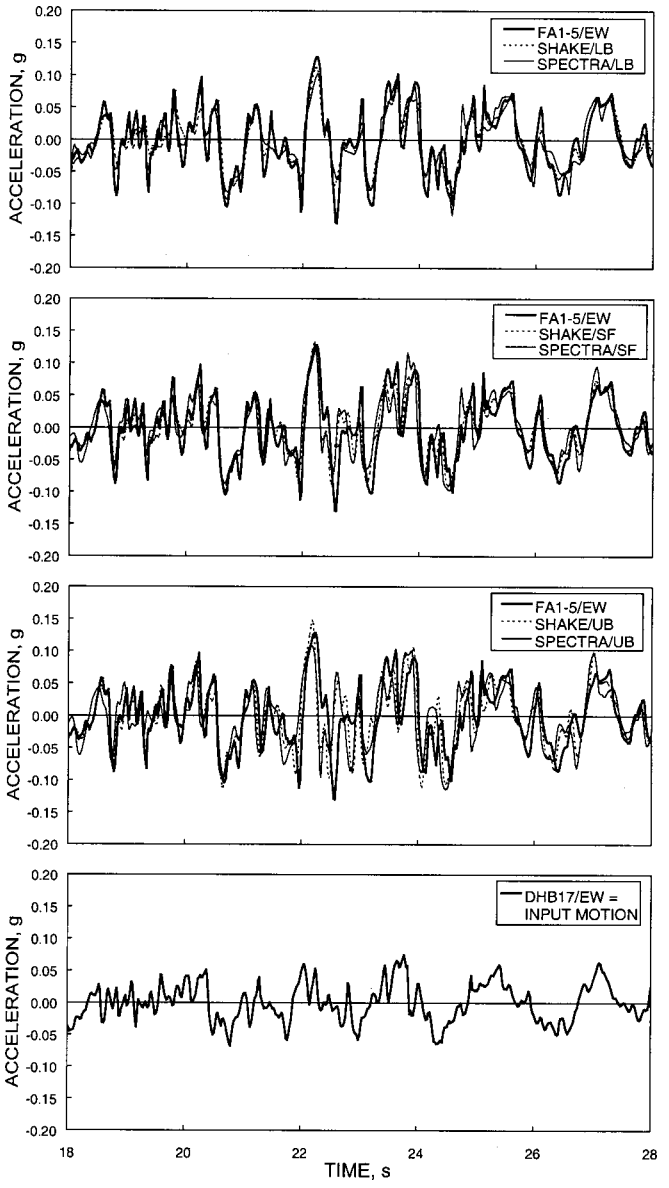


**Fig. 6.** East–West ground surface acceleration-time history using *SHAKE* and *SPECTRA*: Lotung LSST16 case study

Figs. 6 and 7 show predicted and recorded EW and NS ground surface acceleration-time histories for the LSST16 event, as well as the input ground motions at 17 m depth. Only the most significant 10-sec time window is shown to better assess the quality of the time-history predictions. Qualitatively, the predictions of the two codes are better than those for the LSST12 event, particularly with the SF curves, with *SHAKE* overpredicting the EW peak value by 5% and *SPECTRA* underpredicting it by about the same amount. Also, both codes underpredicted the NS peak by less than 5%, although the *SPECTRA* peak did not coincide with the recorded peak. The depth and distance of the earthquake source makes the assumption of vertically propagating waves more appropriate for this earthquake than for the LSST12 earthquake (see Table 1). In fact, it was estimated that even for the relatively closer LSST7 event, the soil layers in Lotung had already bent inclined rays to no more than 6° with the vertical by the time they reached the ground surface (Chang et al. 1990). Thus, for the farther LSST16 event, it is expected that the vertical nature of wave propagation is even more true.

### *Acceleration Response and Fourier Amplitude Spectra*

Figs. 8 and 9 show the horizontal ground surface acceleration response spectra predicted by *SPECTRA* and *SHAKE* along with those recorded during the LSST12 and LSST16 events. It was necessary to assume a damping ratio to construct the response spectra curves, and in Figs. 8 and 9, we have used 5% damping. Qualitatively, there was not much difference between the two sets of predictions, and the SF data curves appear to predict the recorded data quite well. Alternately, Fourier acceleration amplitude spectra are plotted in Figs. 10 and 11, which do not require any assumed damping. In general, peak values of the acceleration response and Fourier acceleration amplitude spectra occur at lower periods (or higher frequencies) during the LSST12 event compared with the LSST16 event.

### *Arias Intensities of Horizontal Ground Motion*

The cumulative Arias intensity $I_a$ is obtained by integrating the square of the acceleration with time and multiplying the result by

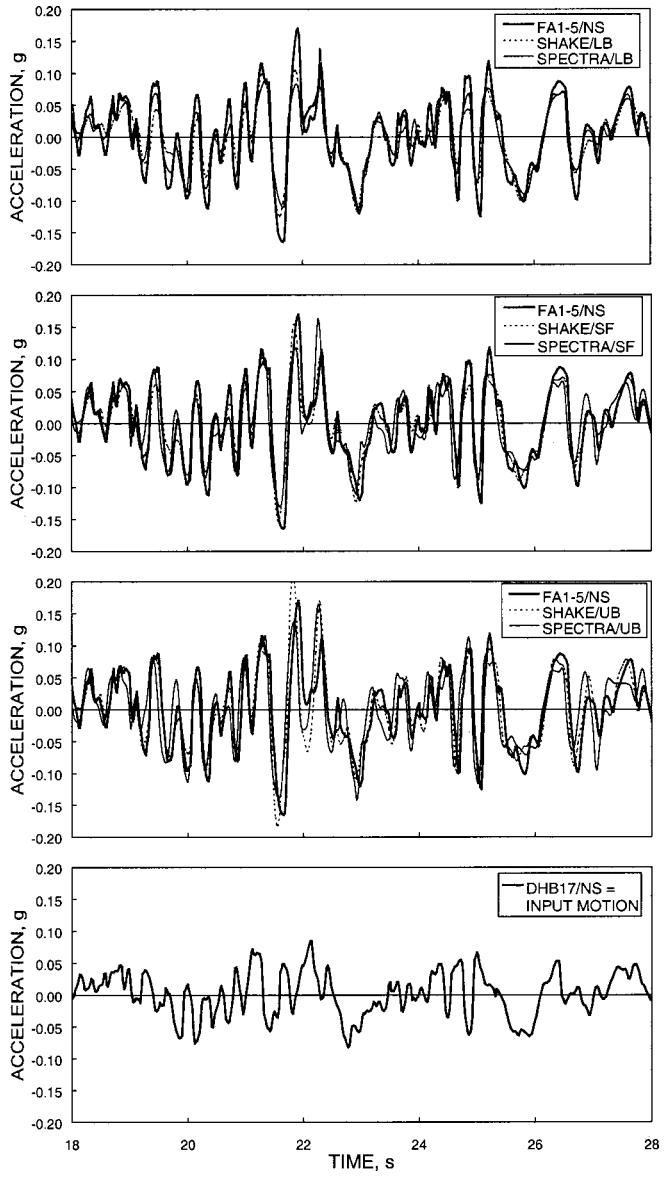


**Fig. 7.** NS ground surface acceleration-time history using *SHAKE* and *SPECTRA*: Lotung LSST16 case study

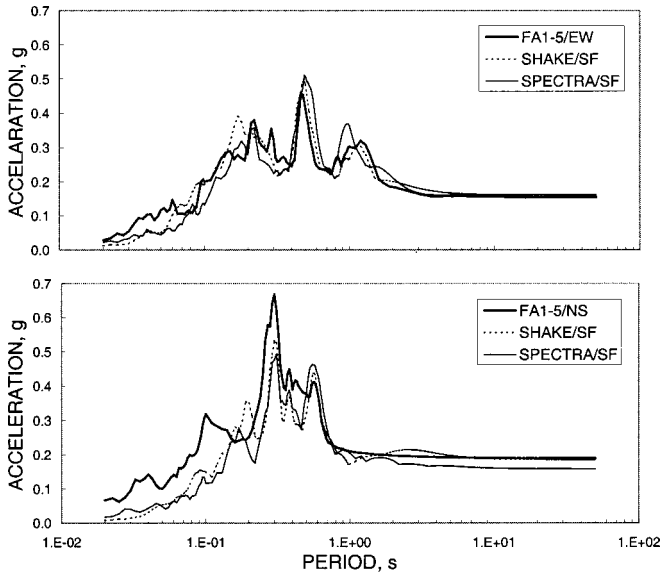


**Fig. 8.** Acceleration response spectra at 5% damping: Lotung LSST12 case study

the constant $\pi/2g$ (Arias 1970), where $g$ is the gravity acceleration constant. This parameter provides a measure of the cumulative energy released by an earthquake as a function of time. Since the resolved acceleration in the horizontal direction follows the relationship $a_h^2=a_{EW}^2+a_{NS}^2$, the Arias intensity of the total horizontal ground motion may be computed as the sum of the Arias intensities of the EW and NS ground motions.

Using $I_a$ as a ground motion parameter, Figs. 12 and 13 compare the Arias intensities of the horizontal ground motions from the LSST12 and LSST16 earthquakes. For the LSST12 earthquake, the intensity calculated by *SPECTRA* using SF curves agrees very well with the intensity of the recorded motion. However, for the LSST16 earthquake, all intensities calculated by the two codes underpredicted the calculated intensity of the recorded motion, although the UB intensity curve generated by *SPECTRA* appears to capture the recorded motion more accurately. Within the range of variations of the moduli ratio considered by the two codes (as well as within the range of variations of the damping ratio considered by *SHAKE*), the ranges of calculated final Arias intensities in 0.001 g-s are as follows. For LSST12, *SHAKE*: $3.4<I_a<5.9$, *SPECTRA*: $3.0<I_a<5.7$; for LSST16, *SHAKE*: $9.9<I_a<12.9$, *SPECTRA*: $9.8<I_a<13.5$.

It must be noted that although *SHAKE* uses both the moduli and damping ratio curves, whereas *SPECTRA* only uses the moduli ratio curve, the *SPECTRA* predictions are at least as accurate as the *SHAKE* predictions, and that both codes have a comparable sensitivity in terms of the range of values of the predicted Arias intensities. In this regard, *SPECTRA* has the advantage that its predictions are influenced only by the uncertainties in the values of the moduli ratio, and not at all by the values of the damping ratio. In fact, *SHAKE*'s dependence on the damping ratio curve has a more negative impact if one considers that data points for damping ratio tend to scatter even more outside of the band considered for the present parametric study (see Fig. 3). If this

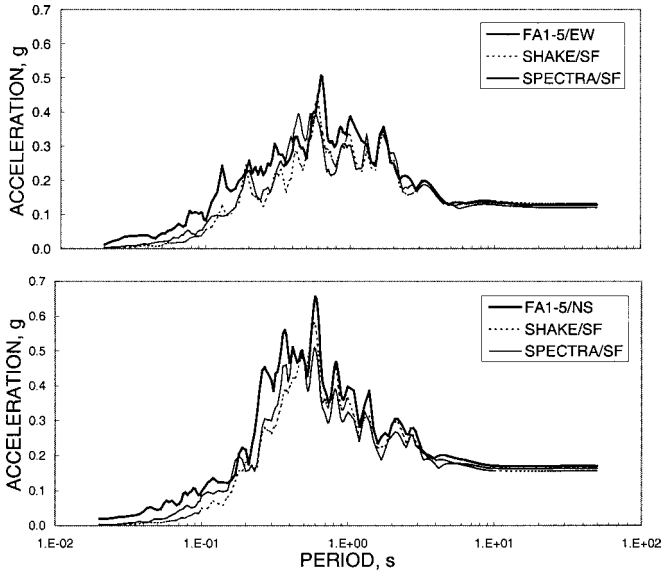


**Fig. 9.** Acceleration response spectra at 5% damping: Lotung LSST16 case study

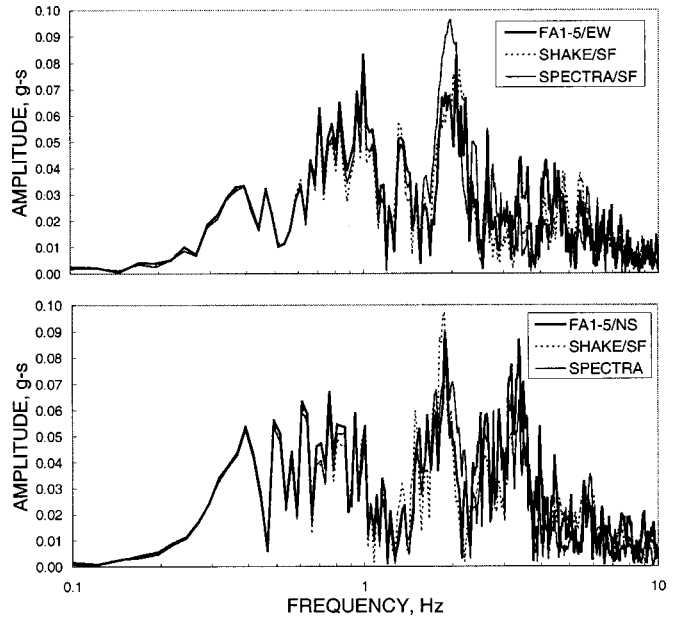


**Fig. 10.** Fourier acceleration amplitude spectra: Lotung LSST12 case study

factor is considered in the sensitivity analysis, it is expected that *SHAKE* will be more vulnerable to statistical variations in the input material properties.

### *Permanent Shear Deformation*

Permanent shear deformations develop in soft soils as a result of intense horizontal ground shaking. In this article, we assess permanent deformations by plotting the time histories of the maximum shear strain developed in the soil column. A plot of the time histories of the maximum shear strain can be constructed by computing, at each time instant, the resolved EW and NS displacements at each nodal point and subtracting the resolved displacements of adjacent nodes to get the relative resolved displacements for each column element. The resolved shear strain can then be obtained by dividing the result by the column thickness (1 m in this case). At each time step, a search for the maximum resolved shear strain can be performed element-by-element, and the result plotted as a function of time to obtain the maximum shear strain history.

Plots of maximum shear strain histories predicted by *SHAKE* and *SPECTRA* during the LSST12 and LSST16 events are shown in Figs. 14 and 15, respectively. Note that both codes predicted maximum shear strains to occur during the period of intense shaking. However, whereas *SPECTRA* predicted persistent maximum shear strains, *SHAKE* predicted maximum shear strains that dissipate with time. The latter, of course, is unrealistic but not surprising since *SHAKE* treats all deformations as recoverable and, therefore, predicts no permanent deformations. The persistent maximum shear strains calculated by *SPECTRA* are on the order of about 0.08% for both the LSST12 and LSST16 events. At this strain level, the shear moduli have degraded to about 30–40% of their initial elastic values (see Fig. 3).

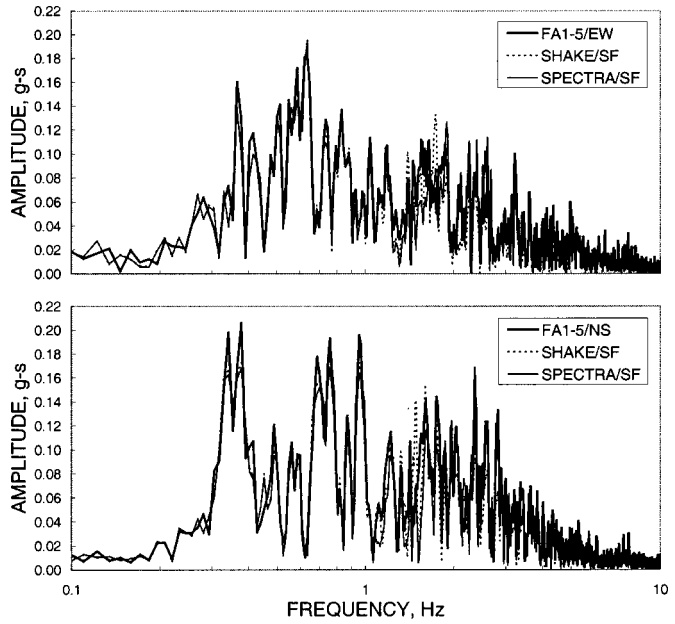


**Fig. 11.** Fourier acceleration amplitude spectra: Lotung LSST16 case study

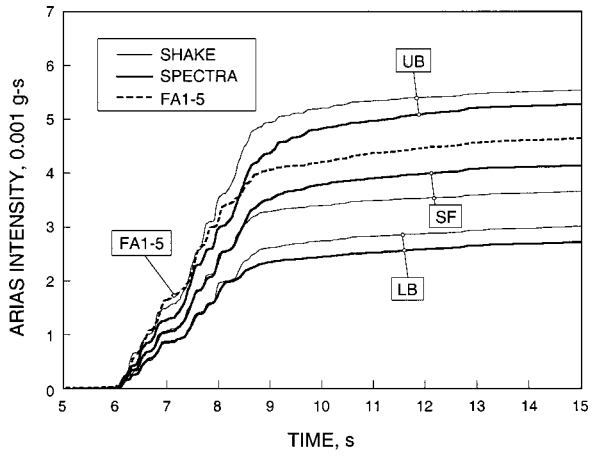


**Fig. 12.** Arias intensities of resolved horizontal ground motion: Lotung LSST12 case study

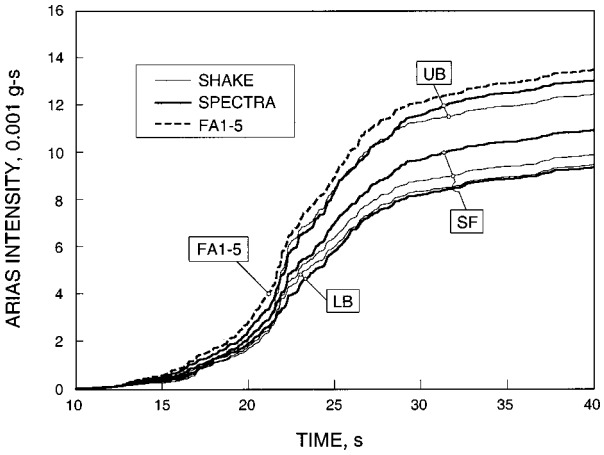


**Fig. 13.** Arias intensities of resolved horizontal ground motion: Lotung LSST16 case study

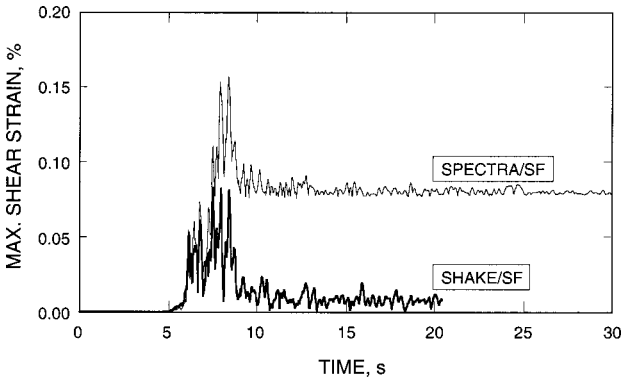


**Fig. 14.** Maximum shear strain history: LSST12 case study

## Summary and Conclusions

Records from two major earthquakes that shook the LSST site in Lotung, Taiwan, have been analyzed using the equivalent linear analysis code *SHAKE* and a recently developed fully nonlinear ground response analysis code *SPECTRA*. The first earthquake had a shorter duration and was near the source (LSST12), while the second earthquake was of longer duration and farther away from the source (LSST16). Based on the statistical curves for material properties back-figured from the same earthquakes, time histories, acceleration response spectra, Fourier acceleration amplitude spectra, and Arias intensities were constructed using the two codes. Both codes predicted the recorded ground surface acceleration responses quite well using the SF curve for shear modulus and damping ratio.

Overall, there was a tendency to underpredict the Arias intensities of the horizontal ground motion when statistical curves for soil properties developed from the *in situ* responses are used as material input data into either code. The results of these studies affirm that natural variations in soil properties can significantly influence the predictions of even the simplest codes such as *SHAKE* and *SPECTRA*. Of course, since *SPECTRA* does not require the damping ratio curve, it is not subject to variations in this particular soil property, an obvious attribute of the new model. In general, care must be taken in developing more complex numerical analysis codes to make sure that systematic procedures are available for determining the required model parameters.

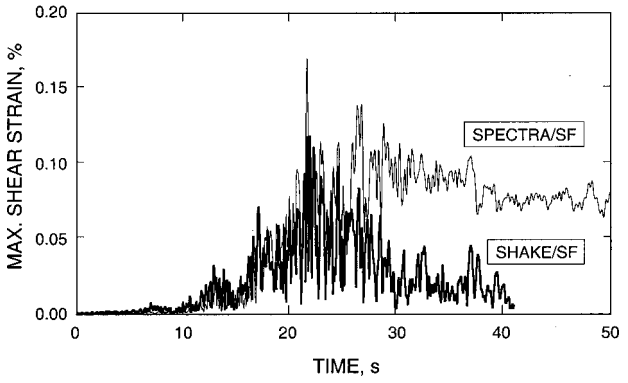


**Fig. 15.** Maximum shear strain history: LSST16 case study

## Acknowledgments

Financial support for this research was provided by the Earthquake Hazard Mitigation Division of National Science Foundation under Contract No. CMS-9613906. The second writer acknowledges financial support provided by the John A. Blume Earthquake Engineering Center. The writers would like to thank Dr. H. T. Tang and Electric Power Research Institute for providing the digitized data for the Lotung earthquakes and the anonymous reviewers for their suggestions.

## References

Anderson, D. G., and Tang, Y. K. (1989). ''Summary of soil characterization program for the Lotung large-scale seismic experiment.'' *Proc. EPRI/NRC/TPC Workshop on Seismic Soil-Structure Interaction Analysis Techniques Using Data from Lotung, Taiwan* EPRI NP-6154, 1, 4.1–4.20.

Arias, A. (1970). ''A measure of earthquake intensity.'' in R. J. Hansen, ed., *Seismic Design for Nuclear Power Plants*, MIT, Cambridge, Mass., 438–483.

Bolt, B. A. (1969). ''Duration of strong motion.'' *Proc. 4th World Conf. on Earthquake Engineering*, Santiago, Chile, 1304–1315.

Borja, R. I., and Amies, A. P. (1994). ''Multiaxial cyclic plasticity model for clays.'' *J. Geotech. Eng.*, 120(6), 1051–1070.

Borja, R. I., Chao, H. Y., Montáns, F. J., and Lin, C. H. (1999a). ''Nonlinear ground response at Lotung LSST site.'' *J. Geotech. Eng.*, 125(3), 187–197.

Borja, R. I., Chao, H. Y., Montáns, F. J., and Lin, C. H. (1999b). ''SSI effects on ground motion at Lotung LSST site.'' *J. Geotech. Eng.*, 125(9), 76–770.

Borja, R. I., Lin, C. H., Sama, K. S., and Masada, G. M. (2000). ''Modelling non-linear ground response of non-liquefiable soils.'' *Earthquake Eng. Struct. Dyn.*, 29, 63–83.

Borja, R. I., Lin, C. H., and Montáns, F. J. (2001). ''Cam-clay plasticity, Part IV. Implicit integration of anisotropic bounding surface model with nonlinear hyperelasticity and ellipsoidal loading function.'' *Comput. Methods Appl. Mech. Eng.*, 190(26–27), 3293–3323.

Chang, C. Y., Mok, C. M., Power, M. S., Tang, Y. K., Tang, H. T., and Stepp, J. C. (1990). ''Equivalent linear and nonlinear ground response analyses at Lotung seismic experiment site.'' *Proc. 4th U.S. National Conf. on Earthquake Engineering*, Palm Springs, Calif., 1, 327–336.

Electric Power Research Institute (1993). ''Guidelines for determining design basis ground motions—Vol. 1: Method and guidelines for estimating earthquake ground motion in Eastern North America.'' *Tech. Rep. No. TR-102293*, Electric Power Research Institute, Palo Alto, Calif.

Hardin, B. O., and Drnevich, V. P. (1972). ''Shear modulus and damping in soils: design equations and curves.'' *J. Soil Mech. Found. Div., Am. Soc. Civ. Eng.*, 98(7), 667–692.

Hilber, H. M., Hughes, T. J. R., and Taylor, R. L. (1977). ''Improved numerical dissipation for time integration algorithms in structural dynamics.'' *Earthquake Eng. Struct. Dyn.*, 5, 283–292.

Idriss, I. M., and Sun, J. I. (1992). *User's Manual for SHAKE91*, Center for Geotechnical Modeling, Univ. of California, Davis, Calif. (November).

Kramer, S. L. (1996). *Geotechnical earthquake engineering*, Prentice–Hall, Engelwood Cliffs, N.J.

Lee, M. K. W, and Finn, W. D. L. (1991). *DESRA-2C: Dynamic effective stress response analysis of soil deposits with energy transmitting boundary including assessment of liquefaction potential*, Univ. of British Columbia, Faculty of Applied Science.

Li, X. S., Wang, Z. L., and Shen, C. K. (1992). *SUMDES: A nonlinear procedure for response analysis of horizontally-layered sites subjected to multi-directional earthquake loading*, Dept. of Civil Engineering, Univ. of California, Davis, Calif.

Li, X. S., Shen, C. K., and Wang, Z. L. (1988). ''Fully coupled inelastic

site response analysis for 1986 Lotung earthquake.'' *J. Geotech. Eng.*, 124(7), 560–573.

Lin, C. H., and Borja, R. I. (2000). *Dynamic theory of mixtures and its finite element implementation for nonlinear analysis of ground motion induced by seismic shaking*, The John A. Blume Earthquake Engineering Center, *Research Rep. No. 137*, Stanford Univ., Stanford, California

Pyke, R. M. (1992). *TESS: A computer program for nonlinear ground response analyses*, TAGA Engineering Systems and Software, Lafayette, Calif.

Schnabel, P. B., Lysmer, J., and Seed, H. B. (1972). *SHAKE—A computer program for earthquake response analysis of horizontally layered sites*, *Rep. No. EERC 72-12*, Univ. of California, Berkeley.

Seed, H. B., and Idriss, I. M. (1970). ''Soil moduli and damping factors for dynamic response analysis.'' *EERC Rep. 70-10*, Univ. of California, Berkeley, Calif.

Shen, C. K., Chan, C. K., Li, X. S., Yang, H. W., Ueng, T. S., Wu, W. T., and Chen, C. H. (1989). ''Pore water pressure response measurements at Lotung site.'' *Proc. EPRI/NRC/TPC Workshop on Seismic Soil-Structure Interaction Analysis Techniques Using Data from Lotung, Taiwan*, Vol. 2, *Rep. No. EPRI NP-6154*, Chapter 25, 1–20.

Tang, H. T., Tang, Y. K., and Stepp, J. C. (1990). Lotung large-scale seismic experiment and soil-structure interaction method validation, *Nucl. Eng. Des.*, 123, 197–412.

Zeghal, M., Elgamal, A. W., Tang, H. T., and Stepp, J. C. (1995). ''Lotung downhole array. II: Evaluation of soil nonlinear properties.'' *J. Geotech. Eng.*, 121(4), 363–378.